Mediterranean Archaeology and Archaeometry, Vol. 16, No. 3, pp. 127-134

10.5281/zenodo.160962

FIRST APPLICATION OF OSL DATING TO A CHALCOLITHIC WELL STRUCTURE IN QULBĀN BANĪ MURRA, JORDAN

Sahar al Khasawneh*[1,3,4], Andrew Sean Murray[2], Hans Georg Gebel[4], Dominik Bonatz[4]

[1]Faculty of Archaeology and Anthropology, Yarmouk University, Jordan
[2]Nordic Laboratory for Luminescence Dating, department of Geoscience, Aarhus University, Denmark
[3]Center for Nuclear Technologies, Risø Campus, Technical University of Denmark, Denmark
[4]Institute for Ancient Near Eastern Archaeology, Free University Berlin, Germany

Received: 22/06/2016
Accepted: 01/09/2016
Corresponding author: Sahar al khasawneh (skhasswneh@yu.edu.jo)

ABSTRACT

This study presents the first OSL dates for a well structure presumed to have been built by pastoralists in Qulbān Banī Murra, Jordan. The site is assumed to belong to the Chalcolithic culture (5th millennium BC). It includes partly megalithic burial fields connected to a water management system. Two sediment samples, composed from reddish silty material used as a hardened lining material for the well structures, were dated using OSL (quartz OSL and feldspar post IR-IRSL). The good agreement between the two chronometers confirms that the sediment was fully reset at the time of burial, and so gives confidence in the reliability of the chronology. The average age derived from quartz of the two samples is 4.6±0.2 Kyr BC and 4.77±0.27 Kyr BC for ages derived from feldspar. Both ages are in agreement with earlier assumptions. These dates represent some of the first instrumental ages for this widespread water-using culture.

KEYWORDS: OSL, well structure, Qulban Bani Murra, megalithic, Jordan

1. INTRODUCTION

Pastoral well-culture occupations make up much of the central parts of the "Mid-Holocene Green Saharo- Arabian Pastoral Belt" (Gebel, 2013), stretching from Yemen to the western Maghreb. The sites are either characterised by extensive megalithic standing-stone burial fields with additional structural features such as ritual structures, well-troughs structures, dams, or by large pens associated with domestic structures (Gebel & Mahasneh, 2012). Taken together, these features give evidence that more humid climate conditions sustained steppe environments used by large mobile shepherd communities, vanishing from 4000 BC when drier periods started. In south-eastern Jordan, Qulban Beni Murra represents a major pastoral burial centre, most probable the focal point of a tribal community commemorating its ancestors and meeting for social transactions. But as in most sites from these cultures, research has always hindered by the difficulty in establishing a robust absolute chronology. The sites are mostly deflated and heavily disturbed by later use or looting. Wells often were re-excavated in all periods, and the 5th millennium BC well bottoms were lost in drier periods as the diggings followed the aquifers at deeper levels. The relative-chronological dating of the site is mainly based on one *fossil directeur*, the "fan scraper"; together with the nature of its structures Qulban Beni Murra can be attributed to the Chalcolithic (Late Chalcolithic/Early Bronze) by comparison with other such evidence from the al-Naqab and Sinai as well as from Rajajil and Rasif in northern Saudi Arabia (Gebel, 2013). In addition to this contextual dating, there is one radiocarbon date on dispersed organics available; this associates the structure with the 2nd half of the 5th millennium BC; (see below). (Gebel & Mahasneh, 2009 and 2012, Gebel, 2010, Gebel *et al.* 2011). Here we use the OSL signals from quartz and post IR-IRSL signals from K-rich feldspar to determine the last time of exposure to daylight of two sediment samples from Qulban Beni Murra site.

2. ARCHAEOLOGICAL SETTING, AGE CONTROL AND SAMPLING

Qulban Beni Murra is located on the shallow and dissected banks of Wadi Sahabal Abyad between 30°03'50"/ 30°05'04"N and 37°14'35"/ 37°15'35"E. some 13 km N of the Saudi border (Figure 1). The immediate site extends for about 1.5 km along both sides of Wadi Sahab al-Abyad, and covers an area of more than one square kilometre- not including outlying grave structures. The wadi banks are shallow *hammada* slopes some 12-14 m above the wadi bottom. The remains of ca. 9 wells/ watering places rest in the wadi floor. The well complex from which the samples were taken (Structure D15) is located in a small mound formed by a mixture of a reddish silty sediment of unknown origin, the structures of the troughs, and the gravels from the well- diggings; the mound is built on the presumed mid-Holocene Wadi floor.

Figure 1. : Location of Qulban Beni Murra in the south-eastern deserts of Jordan. (P. Keilholz).

The ground plan of the watering place (Figure 2) includes a "well room" with a staircase leading to the mouth of the well. The "well room" is joined by stone-paved curvilinear troughs (Spaces 3a-b and 4a-b), as well as two tongue-shaped structures with end rooms (Spaces 7-9 and 10-11, up to 10 m long); the latter apparently are trough lines with descending compartments leading away from the "well room". The paved spaces or troughs were lined and "chambered" by upright (0.5 m) standing stone slabs (Figure 2), and the centre line of the base of these paved spaces reached their highest points close to the mouth of the well. The eroded reddish silty and very compact sediment in which the structural elements of the well/watering complexes are embedded appears to have been the lining material of the troughs; when mixed with water, this sediment hardens to an almost ceramic-like material, The upper part of the well shaft (1.2 m in diameter) is made of corbelled masonry; this rests on well compacted wadi deposits into which small cavities have been set to serve as steps supports. (Gebel & Mahasneh 2012, Gebel, 2013).

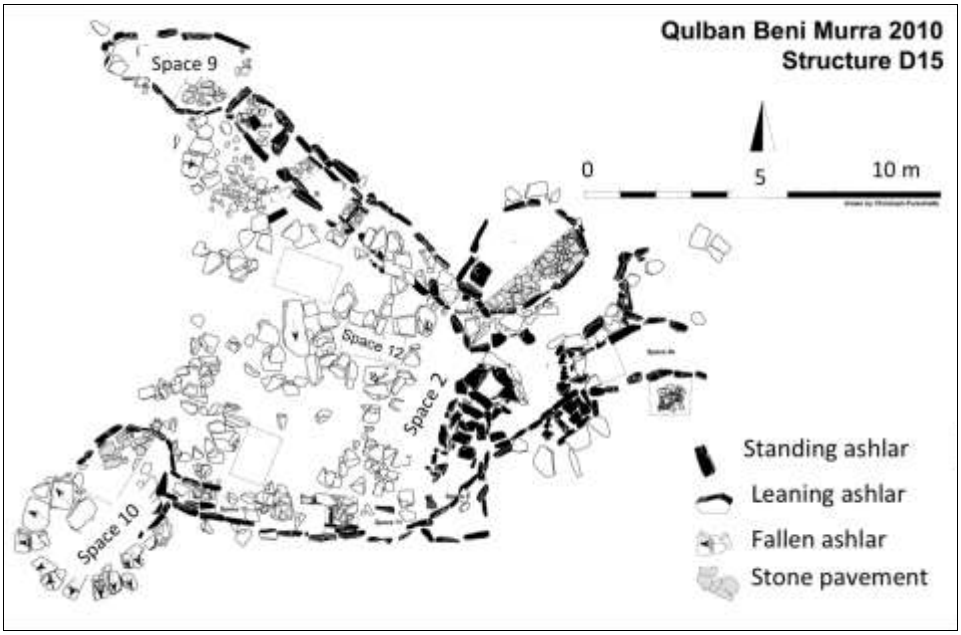

Figure 2. Qulban Beni Murra, Structure D15: Well/watering complex, dated to the 2nd half of the 5th millennium BC. (Field records: Pokrandt/Keilholz, graph: Purschwitz)

This hardened lining/embedding sediment has provided the only independent age control for this site. From a sounding in Space 12 in D15 (Figure 3), sample KIA43373 was taken in 2010 from the lining material, and the disseminated organics within this hardened sediment gave a calibrated ^{14}C age of 4459-4346 cal. BC (2σ range). This date associates the structure with the 2nd half of the 5th millennium BC. (A. Dreves, Leibniz Labor für Altersbestimmung und Isotopenforschung, Kiel University, in letter to J. Pokrandt, Kiel University, pers. comm.)

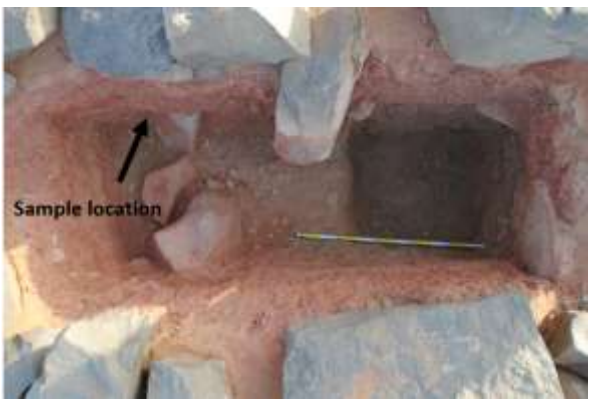

Figure 3. Qulban Beni Murra- Area D, Structure D15- and sample location.

For our study, two OSL sediment samples were taken from the same context of 2010 (sounding in Space 12 in D15) ca. 50 cm below the surface (samples QBM3 and QBM6; laboratory codes BB644 and BB645, respectively).

It remained unclear if this sounding (Figure 3), located about 4 m WNW from the well mouth, was placed in a room or in an open space between two major trough lines. The section did not show any significant stratification, and there were no significant heterogeneities (stones, gravel beds etc.) within 50 cm of the sampling locations. Steel tubes about 1.5 cm internal diameter and 30 cm long were driven into the cleaned face of the section and sealed for transport. The radiocarbon samples were taken from similar neighbouring contexts.

3. SAMPLE PREPARATION AND ANALYTICAL FACILITIES

In the laboratory, the sediment was removed from the tubes under low-level orange lighting. The inner part of the sample was prepared using standard laboratory procedures with dry sieving to separate the fractions 90- 180 µm and 180- 250 µm. Both fractions were treated with 10% HCL to remove carbonates, 30% H_2O_2 to remove organic matter and 10% HF for 20 minutes to remove grain coatings and residual fine material. Aqueous heavy liquid solution (LST Fast float, sodium heteropolytungstate) of density 2.58 $g.cm^{-3}$ was used to separate a quartz-rich fraction from K-rich feldspar grains. Both samples contained only a small amount of feldspar in the grain size range 90- 180 µm and the larger grain size range 180- 250 µm was almost pure quartz. The quartz-rich fractions were then treated with 40% HF for 40 minutes to remove any remaining feldspar and to etch away the alpha-irradiated outer layer of quartz grains.

Grains were mounted on 10 mm diameter stainless steel discs using silicon oil for luminescence measurements.

Luminescence measurements employed an automated Risø TL/OSL-DA20 luminescence reader equipped with a calibrated $^{90}Sr/^{90}Y$ beta source delivering ~0.1 Gy.s^{-1}, blue LEDs (470 nm, ~80 mW/cm^2) and infrared (IR) LEDs (870 nm, ~135 mW/cm^2) (Thompson *et al.*, 2006). Blue light stimulated signals were detected through 7.5 mm of UV Hoya U-340 filter, and signals were calculated by integrating over the first 0.4 s of the quartz stimulation curve less a background derived from the immediately following 0.4 s. IRSL signals were detected through a blue BG-39/7-59 filter combination, and signals were calculated by integrating over the first 20 s of the feldspar stimulation curve less a background derived from the final 10 s.

4. DOSE RATE DETERMINATION

Sediments from the ends of the tube samples were used to estimate gamma and beta dose rate. Water content were first measured and the sediments ignited at 450 °C for 24 hours; they were then homogenised by grinding and mixed with wax before casting in a standard counting geometry (Murray *et al.*, 1987). Radionuclides concentrations (^{238}U, ^{226}Ra, ^{232}Th and ^{40}K) were determined using gamma spectrometry, and converted into dose rates following Guérin *et al.*, (2011). The contribution from cosmic radiation was estimated following Prescott & Hutton (1994), and the burial depths measured in the field (see Table 1).

Table 1. Radionuclide concentrations and resulting dose rates

Sample	Risø code	w.c (%)	^{238}U (Bq/kg)	^{232}Th (Bq/kg)	^{40}K (Bq/kg)	γ-dose rate, (Gy/ka)	β-dose rate, (Gy/ka)	KF- Total dose rate	Qz- Total dose rate
QBM3	BB644	0.2	106±24	23.1±1.7	149±19	0.98±0.07	1.37±0.11	3.07±0.17	2.61±0.12
QBM6	BB645	3.1	102±15	19.1±0.9	165±13	0.92±0.07	1.34±0.08	2.99±0.14	2.42±0.12

5. QUARTZ, LUMINESCENCE CHARACTERISTIC AND SAR PERFORMANCE

Quartz grains were stimulated for 40 s at 125 °C following the conventional SAR OSL protocol presented by Murray & Wintle (2000, 2003). Preheat was fixed at 260 °C for 10 seconds and cut heat to 220 °C for the natural/regenerative dose. OSL signals were measured at 125 °C for 40 seconds. To minimise any possible thermal transfer of charge; blue LED stimulation was given at 280 °C at the end of each cycle. The purity of the quartz grains was tested by IR stimulation at 50 °C for 40 seconds followed by blue LED stimulation at 125 °C for 40 seconds (Duller, 2003).

From a comparison with the OSL curve from calibration quartz (Hansen *et al*., 2015) it can be seen that the natural stimulation curves of the both samples are clearly dominated by the quartz OSL fast component (inset to Figure 4a; Singarayer & Bailey, 2003; Jain *et al.*, 2003). The resulting response of luminescence to dose is shown in Figure 4a; the data have been fitted with a saturating exponential function with characteristic exponential constant D_o=30.08 Gy.

Average recycling ratios and recuperation for sample QBM3 were 0.96±0.04 (n=18) and 10±6% of natural (n=18), respectively. The recycling ratio for sample QBM6 was 1.04±0.04 (n=18) and recuperation 10±3% (n=18). These data demonstrate the reproducibility of measurements made using our SAR protocol when measuring laboratory-induced signals.

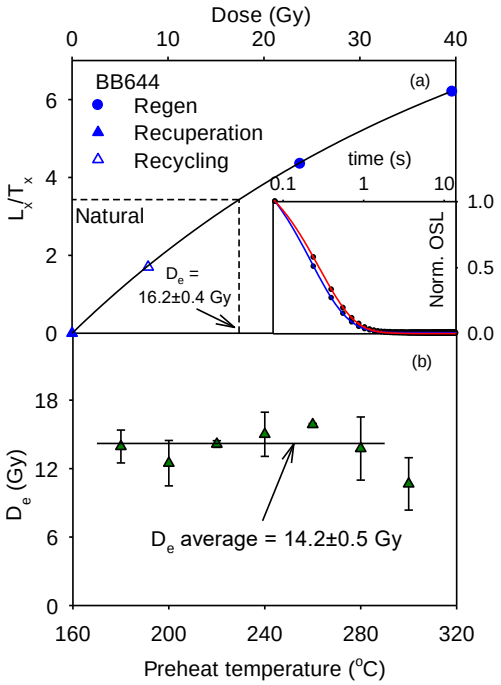

Figure 4. (a) quartz dose-response curve and (inset) a typical decay curve from sample QBM3(BB644). (b) preheat plateau for quartz OSL for the same sample.

We have also tested the dependency of the measured quartz D_e on preheat temperature, by determining equivalent doses using different preheat temperatures between 180 °C and 300 °C (the cut heat was set to be 40 degree less than the

relevant preheat). The results are presented for sample QBM3 in Figure 4b, where it can be seen that there is no significant dependence of the D_e on the preheat temperature.

Finally, a dose recovery test was undertaken to examine the overall performance of SAR protocol. Six aliquots of each sample were illuminated twice using blue light for 100 s at room temperature, the two illuminations separated by storage for 10 ks (also at room temperature) to allow for the thermal decay of the 110 °C trap. The aliquots were then given a dose of ~6 Gy using the beta source and measured in the usual manner. The mean ratio of the measured to the given dose is 1.05 ±0.02 (n=12). This demonstrates that our SAR protocol is able to measure accurately a known dose given to these quartz samples before any thermal treatment. The calculated D_e and the derived ages are summarized in Table 2. The two samples both give ages consistent with the second half of the 5th millennium BC.

6. K- FELDSPAR

6.1.1 pIRIR$_{290}$ luminescence characteristic and SAR performance

Feldspar measurements used the post-IR IRSL single-aliquot regenerative (SAR) protocol as described by Thiel *et al.* (2011). IR stimulation was applied twice, the first stimulation for 100 seconds while the sample was held at 50 °C (IR_{50}), followed by a second stimulation for 100 second while the sample was held at 290 °C ($pIRIR_{290}$). The test dose was chosen to be ~60% of the expected natural dose. Preheat was fixed at 320 °C for both the natural/regenerative and the test dose (Murray *et al.*, 2009). A final IR illumination at 325 °C was applied at the end of each SAR cycle to minimise the thermal transfer of charge to the next cycle (Figure 5).

The reproducibility of the protocol was tested by means of examining the recycling ratio; both samples had ratios close to unity (QBM3= 0.98±0.01 (n=21) and QBM6= 1.005±0.036 (n=21)). The average recuperation, expressed as a fraction of the equivalent dose was: QBM3 $pIRIR_{290}$– 4.01 ±0.19% (n=21); IR_{50}–1.99±0.07% (n=21) and for sample QBM6 $pIRIR_{290}$–3.6±0.11% (n=21); IR_{50}– 1.74±0.07 (n=21).

We next tested the dependence of D_e on the first stimulation temperature for sample QBM3; 18 aliquots were measured in 6 sets of 3 aliquots, with the preheat temperature and the post IRIR stimulation temperature fixed at 320 °C and 290 °C respectively. The temperature of the first IR stimulation started at 50 °C with an increase of 40 °C for each set of 3 aliquots. The same parameter values were used after the test dose in each set. Figure 6 presents the result of this experiment; there is no evident dependence of the D_e derived from either the $pIRIR_{290}$ signal or from the first IR signal on the first stimulation temperature.

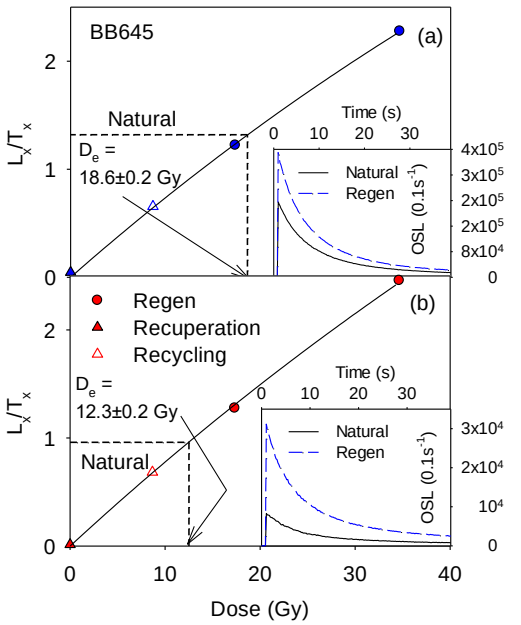

Figure 5. Representative dose response curves and (inset) natural and regenerated stimulation curves for sample QBM6 (BB645) (a) for post-IR IRSL signals stimulated at 290 °C and (b) for IR signals stimulated at 50 °C.

The dependence on preheat was also investigated using sample QBM6. Seven sets, each of three aliquots, were used with a pIRIR protocol in which the preheat temperature was increased from 140 °C to 320 °C in steps of 30 degrees with each set. The first IR stimulation temperature was fixed at 50 °C, and the post IRIR stimulation temperature was chosen to be 30° less than the preheat temperature. Figure 7 shows that the D_e derived from both signals is independent of preheat/pIRIR stimulation temperature over this temperature range.

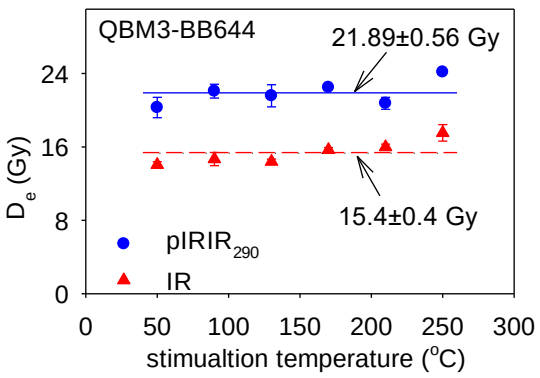

Figure 6. Dependence of D_e values on the first IR stimulation temperature for sample QBM3 (BB644).

Finally, the overall performance of the post IRIR protocol was investigated using a dose recovery test

(Murray, 1996). We chose to apply two different approaches to testing the ability of our protocol to measure a known given dose; the first method was by giving a laboratory dose in addition to the natural dose before any thermal treatment (Murray, 1996).

In this approach, a ~65 Gy dose was given to each of ten aliquots of each sample before any other treatment (i.e. in addition to their natural dose) before measuring the total dose using the $pIRIR_{290}$ SAR protocol. In the same measurement sequence, the natural dose was measured using a further three aliquots of each sample, to provide a reference for the irradiated aliquots.

The ratio of the measured dose (after subtracting the average of the natural dose) to the given dose for $pIRIR_{290}$ was 0.97±0.02 (n=20) and 0.80±0.03 (n=20) for IR_{50} (Figure 8 a, b).

The second method involved; aliquots were reset using light prior to dosing. Twelve aliquots were exposed under a Hönle SOL2 solar simulator for 5 hours at a distance of 80 cm. An ~22 Gy dose was then given to each aliquot before measuring using the $pIRIR_{290}$ protocol. The average ratio for the measured to the given dose ($pIRIR_{290}$) was 1.01±0.09 (n=24) and 0.69±0.02 for IR_{50} (Figure 8 c, d).

The results from both methods indicate that our SAR protocol is able to measure accurately a known dose given before any thermal or radiation treatment.

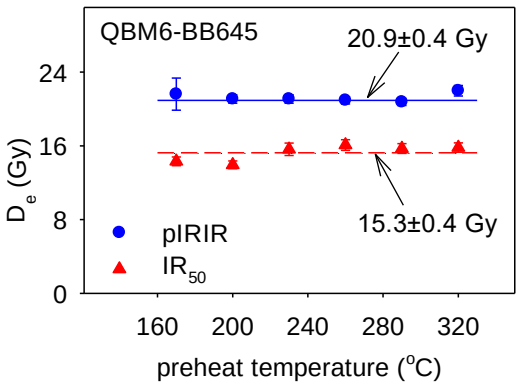

Figure 7. The relationship between the apparent equivalent dose and preheat temperature for sample QBM6 (BB645).

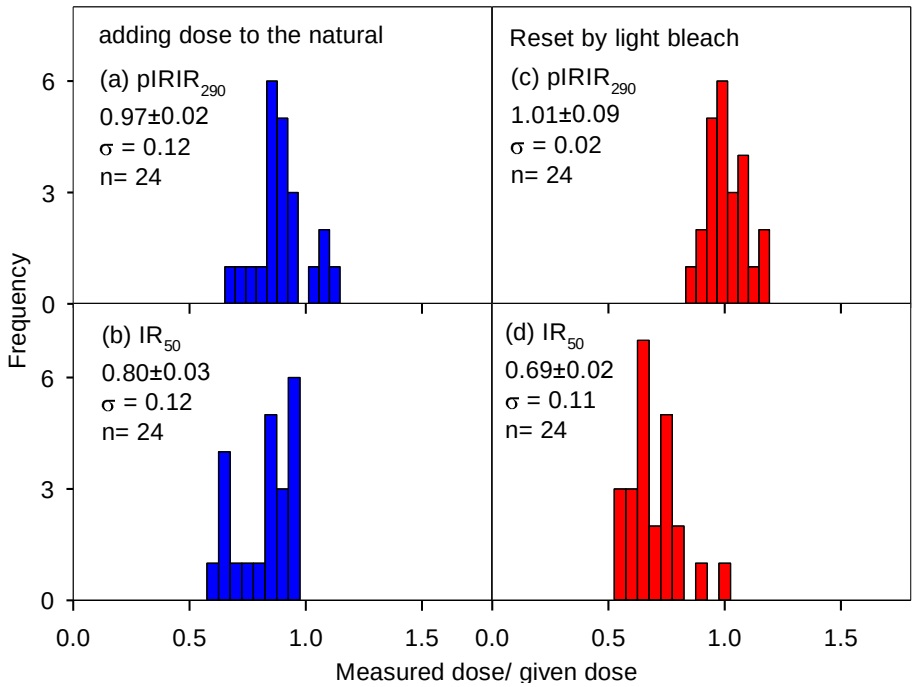

Figure 8. Dose recovery measurements. Ratios of measured dose to given dose for both $pIRIR_{290}$ and IR_{50} signals in dose recovery measurements for feldspar: (a,b) Samples measured after adding external dose to their natural dose, (c,d) samples exposed in solar stimulator for 4 hours before giving laboratory dose.

6.1.2 Fading rate measurement

Anomalous fading is the loss of luminescence with time exhibited by certain minerals for which kinetic studies have shown that the signal should remain stable (see Aitken, 1985, Appendix F). The most widely accepted explanation for anomalous fading is that electrons tunnel from traps to nearby recombination centres without passing through the conduction band. It is been shown by several studies that the signal loss can be approximated by a logarithmic decay (Huntley & Lamothe, 2001, Auclair *et al.*, 2003). It is thus convenient to express the fading rate as the percentage of signal lost during a storage period of one decade of time (the g-value) where the storage periods are expressed as decades relative to the laboratory irradiation period.

We have measured the laboratory fading for both samples; g-values were derived using the sensitivity-corrected IRSL signal after various periods of storage (Lamothe *et al.* 2003) (Table 2). The average g-value for the $pIRIR_{290}$ signal is 0.87±0.17%/decade (n=12), and the average g-value for the IR_{50} signal is 5.2±2.2%/decade (n=12); this difference is expected since the IR_{50} signal is known to be less stable than the $pIRIR_{290}$ signal (e.g. Thompson *et al*. 2011).

6.1.3 D_e and IR ages

The D_e values for the IR_{50} and $pIRIR_{290}$ signals are shown in Table 2, together with the derived ages. Those based on the $pIRIR_{290}$ signal do not involve a fading correction (see e.g. Buylaert et al., 2012), whereas those based on the IR_{50} signal are corrected using the 'g' values shown and the equation of Huntley and Lamothe (2001).

7. DISCUSSION AND CONCLUSIONS

Table 2 summarise the derived luminescence ages for the two samples from OSL quartz, $pIRIR_{290}$ and the corrected ages for the IR_{50} from feldspars. The two samples give the same ages within one sigma of error. The ratio of the corrected IR_{50} ages to the $pIRIR_{290}$ ages confirm that measuring at elevated temperature had minimised the loss of the signal due to anomalous fading.

OSL dating from quartz and $pIRIR_{290}$ from feldspar strongly support the archaeological age for the site. And the available ^{14}C date supports the OSL ages. It also shows that despite the lack of a stratigraphic sequence, their deposition of sediments as a result of human activity was sufficient to reset the luminescence signal (as demonstrated by the agreement between feldspar and quartz ages). These satisfactory results support the potential of using luminesce dating for geo-archaeological landscapes, where the nature of these sites and the lack of organic matter had hindered the development of reliable chronologies.

Table 2. Quartz and feldspars ages (Kyrs BC).

Sample	Risø code	D_e, (Gy)			g- value (%/decade)		Age (BC)		
		Qz	$pIRIR_{290}$	IR_{50}	$pIRIR_{290}$	IR_{50}	Qz	$pIRIR_{290}$	Corrected IR_{50}
QBM3	BB644	16.4±0.8	20.0±0.4	12.5±0.3	1.0±0.3	4.8±0.9	4.4±0.5	4.5±0.4	4.2±0.8
QBM6	BB645	16.4±0.8	21.0±0.4	12.5±0.2	0.7±0.2	5.7±1.0	4.8±0.5	5.0±0.4	5.1±1.1

REFERENCES

Aitken, M. J. (1985). *Thermoluminescence dating* . London: Academic Press.

Auclair, M., Lamothe, M., & Huot, S. (2003). Measurement of anomalous fading for feldspar IRSL using SAR. *Radiation Measurements, 37*, 487-492.

Buylaert, J., Jain, M., Murray, A. S., Thomsen, K., Thiel, C., & Sohbati, R. (2012). A robust feldspar luminescence dating method for Middle and Late Pleistocene sediments. *Boreas, 41*, 435–451.

Duller, G. (2003). Distinguishing quartz and feldspar in single grain luminescence measurements. *Radiation Measurements, 37*, 161-165.

Gebel , H., & Mahasneh, H. (2013). Disappeared by climate change: the shepherd cultures of Qulban Beni Murra (2nd half of the 5th millennium BC) and their aftermath." Syria. *revue d'art oriental et d'archéologie, 90*, 127-158.

Gebel, H. (2010). Untergegangen im Klimawandel. Die paläo-beduinische Kultur von Qulban Beni Murra, Jordanien . *Antike Welt , 6*(10), 40-44.

Gebel, H. (2013). Arabia's fifth-millennium BCE pastoral well cultures: hypotheses on the origins of oasis life. *Proceedings of the Seminar for Arabian Studies, 43*, 111-126.

Gebel, H., & Mahasneh, H. (2009). Petroglyphs and sepulchral contexts, Preliminary note on late Chalcolithic/early Bronze Age findings at Qulban Beni Murra, Wadi Sahab al-Abyad . *Journal of Epigraphy and Rock Drawing , 3*, 1-9.

Gebel, H., & Mahasneh, H. (2012). Qulban Beni Murra. Unknown Mid-Holocene Sepulchral Green Desert Landscapes, Pastoral Well Cultures, and the Origins of Arabia's Oasis Economies. In R. Eichmann, F. Klimscha, C. Schuler, & H. Fahlbusc (Eds.), *Wasserwirtschaftliche Innovationen im archäologischen Kontext. Von den prähistorischen Anfängen bis zu den Metropolen der Antike* (pp. 101-122). Rahden, Leidorf.

Gebel, H., Mahasneh, H., Keilholz , P., & Baumgarten, J. (2011). Life at the edge: Sepulchral, hydraulic and pastoral land use in Wādīs as-Sahab al-Abyad and al-Asmar, southeastern Jordan. Preliminary report of the Eastern Jafr J.A.P., 4th Season, 2010. *Annual of the Department of Antiquities, 55*, 537-559.

Guérin, G., Mercier, N., & Adamiec, G. (2011). Dose-rate conversion factors: update. *Ancient TL , 29*(1), 5-8.

Hansen, V., Murray, A., Buylaert, J., Yeoa, E., & Thomsen, K. (2015). A new irradiated quartz for beta source calibration. *Radiation Measurements, 81*, 123-127.

Huntley, D., & Lamothe, M. (2001). Ubiquity of anomalous fadingin K-feldspars and the measurement and correction for it in optical dating. *Canadian Journal of Earth Science, 38*, 1093/ 1106.

Jain, M., Murray, A., & Bøtter-Jensen, L. (2003). Characterisation of blue-light stimulated luminescence components in different quartz samples: implications for dose measurement. *37*(4), 441-449.

Lamothe, M., Auclair, M., Hamzaoui, C., & Huot, S. (2003). Towards a prediction of long-term anomalous fading of feldspar IRSL. *Radiation Measurement, 37*, 493–498.

Murray, A. S. (1996). Developments in optically transferred luminescence and photo-transferred thermoluminescence dating: application to a 2000-year sequence of flood deposits. *Geochimica et, 60*, 565-576.

Murray, A. S., & Wintle, A. G. (2000). Luminescence dating of quartz using an improved single-aliquot regenerative-dose protocol. . *Radiation Measurements, 32*, 57-73.

Murray, A. S., Buylaert, J. P., Thomsen, K. J., & Jain, M. (2009). The effect of preheating on the IRSL signal from feldspar. *Radiation Measurements, 44*, 554-559.

Murray, A., & Wintle, A. (2003). The single aliquot regenerative dose protocol: Potential for improvements in reliability. *Radiation Measurements, 37*, 377-381.

Murray, A., Marten, R., Johnston, A., & Martin, P. (1987). Analysis for naturally occuring radionuclides at environmental concentrations by gamma spectrometry. *Journal of Radioanalytical and Nuclear Chemistry, 115*(2), 263-288.

Prescott, J. R., & Hutton, J. T. (1994). Cosmic ray contributions to dose rates for luminescence and ESR dating: large depths and long-term variations. *Radiation Measurements, 23*, 497-500.

Singarayer, J., & Bailey, R. (2003). Further investigations of the quartz optically stimulated luminescence components using linear modulation. *Radiation Measurements , 37*(4), 451-458.

Thiel, C., Buylaert, J. P., Murray, A. S., Terhorst, B., Hofer, I., Tsukamoto, S., & Frechen, M. (2011). Luminescence dating of the Stratzing loess profile (Austria) - Testing the potential of an elevated temperature post-IR IRSL protocol. *Quaternary International, 234*, 23- 31.

Thomsen , K., Bøtter-Jensen, L., Denby , P., Moska , P., & Murray, A. (2006). Developments in luminescence measurement techniques. *Radiation Measurements , 41*, 768-773.

Thomsen, K., Murray, A., & Jain, M. (2011). Stability of IRSL signals from sedimentary K-feldspar samples. *Geochronometria, 38*, 1-13.